

**TRANSPORT THROUGH CARBON STEEL OF HYDROGEN
PRODUCED BY FLOW-ACCELERATED CORROSION**



Prisana Homhuandee

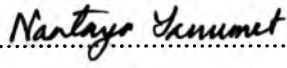
A Thesis Submitted in Partial Fulfilment of the Requirements
for the Degree of Master of Science
The Petroleum and Petrochemical College, Chulalongkorn University
in Academic Partnership with
The University of Michigan, The University of Oklahoma,
Case Western Reserve University and Institut Français du Pétrole

2008

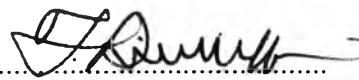
512015


Thesis Title: Transport Through Carbon Steel of Hydrogen Produced by
Flow-Accelerated Corrosion
By: Prisana Homhuandee
Program: *Petroleum Technology*
Thesis Advisors: Assoc. Prof. Thirasak Rirksomboon
Prof. Frank R. Steward
Mr. Andy Justason

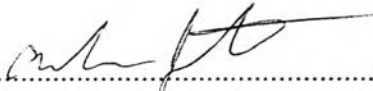
Accepted by the Petroleum and Petrochemical College, Chulalongkorn University, in partial fulfilment of the requirements for the Degree of Master of Science.

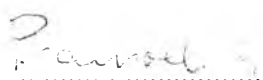

..... College Director
(Assoc. Prof. Nantaya Yanumet)

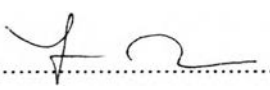
Thesis Committee:


.....
(Assoc. Prof. Thirasak Rirksomboon)


.....
(Prof. Frank R. Steward)


.....
(Mr. Andy Justason)


.....
(Assoc. Prof. Pramoch Rangsunvigit)


.....
(Dr. Boonrod Sajjakulnukit)

ABSTRACT

4973006063: Petroleum Technology Program
Prisana Homhuandee: Transport Through Carbon Steel of Hydrogen
Produced by Flow-Accelerated Corrosion
Thesis Advisors: Assoc. Prof. Thirasak Rirksomboon, Prof. Frank R.
Steward, and Andy Justason, 105 pp.
Keywords: Hydrogen Probe/ Flow-Accelerated Corrosion/ Oxide Films/
Corrosion Monitoring/ Hydrogen Evolution

Atomic hydrogen is produced as a by-product when a ferrous metal surface is exposed to water at a high temperature at a rate corresponding to the rate of corrosion. In de-aerated conditions, the hydrogen atoms permeate through the steel and combine into pairs to form molecular hydrogen at the opposite surface. Because of rapid diffusion of hydrogen through ferrite steels at the temperature of interest, the total rate of hydrogen emission from the steel is a measurement of the instantaneous corrosion rate. The Hydrogen Effusion Probe (HEP) has been developed for an on-line monitor of Flow Accelerated Corrosion (FAC) by measuring the generated through-wall hydrogen. This study was carried out to investigate the transport of hydrogen through steel to obtain a fundamental understanding of the through-wall hydrogen behaviour. HEPs have been installed on a feeder pipe in the Point Lepreau Generating Station (PLGS), on a boiler wall in the Coleson Cove Generating Station (CC), and in a test loop at the Centre Nuclear Energy Research (CNER) laboratory. Data from PLGS, CC and the experiments indicate that the HEP is sensitive and responsive to changes in FAC rate, and can provide an on-line monitor of FAC.

บทคัดย่อ

ปริศนา หอมหวลดี : ชื่อหัวข้อวิทยานิพนธ์ การแพร่ของไฮโดรเจนที่เกิดจากการกัดกร่อนแบบเร่งด้วยความเร็วของของไหลผ่านเหล็กคาร์บอน (Transport Through Carbon Steel of Hydrogen Produced by Flow-Accelerated Corrosion) อ. ที่ปรึกษา : รศ.ดร. ชिरศักดิ์ ฤกษ์สมบูรณ์, ศ.ดร. แฟรงค์ อาร์ สจีวิต และ แอนดี จัสเตชัน, 105 หน้า

ไฮโดรเจนอะตอมเป็นผลิตภัณฑ์ข้างเคียงที่เกิดขึ้นเมื่อพื้นผิวของเหล็กสัมผัสกับน้ำที่อุณหภูมิสูงซึ่งอัตราการเกิดของไฮโดรเจนอะตอมจะสัมพันธ์กับอัตราการกัดกร่อนของเหล็ก ในสถานะที่ปราศจากออกซิเจน ไฮโดรเจนอะตอมที่เกิดขึ้นจะแพร่ผ่านเหล็กแล้วจึงรวมตัวกันเป็นไฮโดรเจนโมเลกุลที่บริเวณพื้นผิวอีกด้านหนึ่ง เนื่องจากไฮโดรเจนอะตอมสามารถแพร่ผ่านเหล็กได้อย่างรวดเร็วในช่วงอุณหภูมิที่พิจารณา ดังนั้นการวัดอัตราการแพร่รวมของไฮโดรเจนเปรียบเสมือนการวัดอัตราการกัดกร่อนในขณะนั้น เครื่องมือวัดการแพร่ผ่านของไฮโดรเจน (Hydrogen Effusion Probe, HEP) ได้รับการพัฒนาขึ้นเพื่อใช้สำหรับตรวจวัดการกัดกร่อนแบบเร่งด้วยความเร็วของของไหล (Flow Accelerated Corrosion, FAC) โดยตรง โดยการวัดปริมาณไฮโดรเจนที่เกิดขึ้นภายในและแพร่ผ่านออกมาจากผนังของโลหะ งานวิจัยนี้ได้ทำการศึกษาหลักการพื้นฐานของพฤติกรรมการแพร่ของไฮโดรเจนผ่านโลหะ โดยได้นำเครื่องมือวัดการแพร่ผ่านของไฮโดรเจนไปติดตั้งที่ท่อแลกเปลี่ยนความร้อนในโรงผลิตไฟฟ้า พอยท์ ลาโพ (Point Lepreau Generating Station) ตรงผนังท่อน้ำร้อนในโรงผลิตไฟฟ้า โคลสัน โคว์ฟ (Coleson Cove Generating Station) และกับท่อในระบบจ่ายของศูนย์วิจัยพลังงานปรมาณู (Centre for Nuclear Energy Research) ประเทศแคนาดา ข้อมูลที่ได้จากโรงผลิตไฟฟ้าทั้งสองและจากการทดลองพบว่าเครื่องมือวัดการแพร่ผ่านของไฮโดรเจนมีความไวและตอบสนองต่อการเปลี่ยนแปลงของอัตราการกัดกร่อนแบบความเร่งด้วยความเร็วของของไหล และใช้เป็นเครื่องตรวจวัดการกัดกร่อนแบบดังกล่าวได้โดยตรง

ACKNOWLEDGEMENTS

The author is grateful for the scholarship and funding of the thesis work provided by the Petroleum and Petrochemical College; and the National Center of Excellence for Petroleum, Petrochemicals, and Advanced Materials, Chulalongkorn University.

I would like to express my deep gratitude to my advisor, Prof. Frank R. Steward and Assoc. Prof. Thirasak Rirksomboon who gave me an opportunity to carry out my research at University of New Brunswick, Canada. It was such a priceless experience for me. I would like to thank them for their knowledge and advice as well.

The intensive suggestions, valuable guidance, and vital help throughout this research work of Prof. Frank R. Steward, Mr. Andy Justason, and Prof. Derek H. Lister will not be forgotten. I would not achieve this project without their assistance.

Big thank goes to Mr. Bob Crawford and Mr. Andrew Feicht for letting me learn many things from your experience, and for making my work here a lot easier otherwise my project would not be completed.

I would like to thank all staff of the Centre for Nuclear Energy Research (CNER) especially the chemical research group for providing the laboratory facilities, and all data from the plants with enormous support and expertise.

Much happiness came from my incredible friends in Fredericton, Canada, I would like to thank them for always standing beside me, making me feel like home, and cheering me up.

Many thanks are due to my friends in Thailand for a warm support and giving me the valuable encouragement.

Last but not least, I would like to express my sincere appreciation to my parents for always believe in me. Your unconditional love and devotion help me get through all troubles. Without you, I am nobody at all.

TABLE OF CONTENTS

	PAGE
Title Page	i
Abstract (in English)	iii
Abstract (in Thai)	iv
Acknowledgements	v
Table of Contents	vi
List of Tables	x
List of Figures	xi
Abbreviations	xv
List of Symbols	xvi
 CHAPTER	
I INTRODUCTION	1
 II THEORETICAL BACKGROUND AND LITERATURE REVIEW	 3
2.1 CANDU Nuclear Reactor	3
2.1.1 CANDU Primary Coolant Loop	4
2.1.2 Feeder Pipe Material and Conditions	5
2.2 Coleson Cove Generating Station	6
2.2.1 Steam Generators	6
2.2.2 Boiler Water Walls Tubing	7
2.2.3 Boiler Blowdown	8
2.3 Corrosion of Steel	8
2.3.1 Definition of Corrosion	8
2.3.2 Corrosion of Steel in Water System	8
2.3.3 Flow-Assisted Corrosion (FAC)	9
2.3.4 FAC on the Feeder Pipe of CANDU Reactor	10
2.4 The Effect of Temperature on the Corrosion Rate	11

CHAPTER	PAGE
2.5 Corrosion Mechanism and Hydrogen Evolution	14
2.5.1 Mechanism of Oxide Growth	14
2.5.2 Hydrogen Emission during Steel Corrosion	18
2.6 The Fundamental Law of Diffusion	18
2.6.1 Fick's Law of Diffusion	19
2.6.1.1 Fick's First Law	19
2.6.1.2 Fick's Second Law	20
2.6.2 Henry's Law and Sievert's Law	21
2.6.3 Arrhenius Equation	23
2.6.4 Graham's Law of Effusion	24
2.7 Hydrogen Diffusion through Metal	26
2.7.1 Mechanism of Hydrogen Transport through Metal	26
2.7.2 Hydrogen Diffusivity Determination Methods	27
2.7.2.1 Steady-State Flow Method	28
2.7.2.2 Hydrogen Absorption	28
2.7.2.3 Time Lag Method	28
2.7.2.4 Electro Chemical Method	28
2.7.2.5 Internal Friction Method	28
2.7.2.6 Hydrogen Microprint Technique (HMT)	29
2.7.3 Hydrogen Diffusivity in Iron	29
2.7.4 Hydrogen Permeability in Iron	33
2.7.5 Hydrogen Diffusivity in Oxide Film	34
2.7.6 Hydrogen Diffusivity in Iron Alloys	35
2.7.6.1 Fe-Al Alloy	35
2.7.6.2 Fe-Ni Alloy	36
2.7.6.3 Fe-Cr Alloy	38
2.8 Hydrogen Solubility in Iron	39
2.9 Hydrogen Damage	42
2.9.1 Hydrogen blistering	42
2.9.2 Hydrogen embrittlement	42

CHAPTER	PAGE
2.9.3 Decarburization and Hydrogen Attack	42
2.10 Hydrogen Probe for Monitoring Corrosion	43
2.10.1 Hydrogen Probe Principle	43
2.10.2 Comparing HEP to FOLTM (Conventional Device)	45
2.11 Former Experiments on the Hydrogen Probe	45
2.11.1 Hydrogen Patch Probe	45
2.11.2 Hydrogen Vacuum Foil or Beta Foil	46
2.11.3 Hydrogen Effusion Probe (HEP)	47
 III EXPERIMENTAL	 50
3.1 Materials	50
3.2 Equipments	51
3.3 Experimental Procedures	52
3.3.1 Study of the Effect of Temperature and Hydrogen Transport	52
3.3.2 Theoretical Studies and Plant Data Analysis	53
3.4 Assumptions for Thinning Rate Measurement by the HEP	54
 IV RESULTS AND DISCUSSION	 55
4.1 Thermodynamics Equilibrium	55
4.2 Hydrogen Transport Through Solid	57
4.2.1 Mathematics of Hydrogen Diffusion	57
4.2.2 The Breakthrough Time of Hydrogen Diffusion	60
4.2.3 Estimation of Hydrogen Diffusivity by the Time Lag Method	61
4.3 Hydrogen Monitoring at the Coleson Cove	63
4.3.1 Effect of the Load of the boiler	63
4.3.2 Effect of the pH of the Solution	65
4.3.3 Boiler Blowdown (Opened/Closed)	66

CHAPTER	PAGE
4.4 Hydrogen Transport through the Pressure Transducer Diaphragm	67
4.5 Prediction of Hydrogen Permeation and Accumulation	71
4.6 The HEP Experiment in Loop 1	76
4.7 Oxygen in the Water Solution	83
4.8 The Effect of Capillary Tube Length on the Response Time	85
V CONCLUSIONS AND RECOMMENDATIONS	87
5.1 Conclusions	87
5.2 Recommendations	88
REFERENCES	89
APPENDICES	95
Appendix A Thermodynamic Equilibrium Calculations	95
Appendix B Diffusion Coefficient by Time-Lag Method	97
Appendix C Hydrogen Diffusion Through the Pressure Transducer Diaphragm	98
C.1 Using Fick's Equation	98
C.2 Using the Permeability Equation	99
Appendix D Average Hydrogen Diffusion Coefficient of Iron	100
Appendix E Solubility of Oxygen in the Solution	101
Appendix F Hydrogen Permeation	102
CURRICULUM VITAE	105

LIST OF TABLES

TABLE		PAGE
2.1	Normal outlet feeder conditions at Point Lepreau Generating Station	5
2.2	Data of hydrogen permeability in iron (S.A. Steward, 1983)	34
3.1	Chemical composition of carbon steel ASME SA106	51
3.2	Loop 1 process parameters	52
A.1	Thermodynamics properties (Perry's Handbook)	95
F.1	Composition of carbon steel ASME SA106 and ASTM A179	103
F.2	The change of pressure inside the tube	104

LIST OF FIGURES

FIGURE	PAGE
2.1 Schematic of a CANDU nuclear reactor.	3
2.2 Primary coolant system of CANDU reactor (Emoscopes, 2006).	4
2.3 Integral furnace industrial boiler for oil and gas firing (Babcock and Wilcox, 1972).	6
2.4 Boiler water walls tubing.	7
2.5 Simplified mechanism for FAC (M. D. Silbert, 2002).	10
2.6 Flow and temperature dependence of single-phase FAC for ammonia solution with a room temperature of 9.04 (Chexal <i>et al.</i> , 1996).	11
2.7 Temperature and dissolved oxygen (DO) diagram (K. Mabuchi, 1991).	12
2.8 Oxidation of mild steel in 13% NaOH at five different temperatures plotted against square root time is on the left, and on the right shows variation with reciprocal absolute temperature of logarithm of the parabolic growth constant (Potter and Mann, 1962).	12
2.9 Sweenton and Baes iron solubility results (L.L. Lang, 1996).	13
2.10 Dependence of the corrosion rate of metals steels, and alloys on temperature of concentrated sulfuric acid (É. T. Shapovalov, 1994).	14
2.11 Schematic of carbon steel corroding in coolant under-saturated in dissolved iron (Lister <i>et al.</i> , 2001).	15
2.12 SEM of oxide film formed under flow condition at 10.000X magnification (T. Pattanaparadee, 2007).	16
2.13 A schematic view of the formation mechanism of the magnetite film on the steel surface in high-temperature water (Cheng and Steward, 2004).	17
2.14 Effusion of gas through a tiny pore or pinhole into a vacuum.	19
2.15 Arrhenius plot of diffusion constant.	24

FIGURE	PAGE
2.16 The time required for different gasses to diffuse through a vacuum.	25
2.17 Seven steps of hydrogen permeation (M.G. Matei, 1999).	27
2.18 Diffusion coefficient of hydrogen through α -iron.	30
2.19 Arrhenius plot of hydrogen diffusion coefficient for α -iron.	30
2.20 The dependence of hydrogen diffusivity on membrane thickness.	33
2.21 Diffusion coefficient of hydrogen as a function of composition at different temperatures (W. Beck et al., 1971).	37
2.22 Diffusion coefficient of hydrogen through α -Iron and its alloys.	39
2.23 Solubility of hydrogen in α -iron (V.I. Tkachev et al., 1979).	40
2.24 Temperature dependence of hydrogen solubility in pure iron at 1 atm pressure (W.Y. Choo, et al. 1981).	41
2.25 Hydrogen patch probe configurations (H. Bruce Freeman, 1994).	46
2.26 Beta Foil configurations (Matei, D.G. 1999).	47
2.27 Schematic of HEP Assembly (McKeen, 2007).	48
2.28 The HEP (top) and FOLTM (bottom) installed on feeder pipe at PLGS (McKeen, 2007).	49
3.1 Configurations of the Hydrogen Effusion Probe, HEP; the HEP installed on the test section of Loop 1 at CNER (left), and the HEP installed on the feeder tube walls at Coleson Cove (right).	50
3.2 Schematic diagram of the CNER Test Loop 1.	52
4.1 The graph relationship between ratio of hydrogen to water partial pressure and temperature.	56
4.2 Concentration distributions at various times with initial uniform concentration C_0 and surface concentration C_2 at one side, zero at the opposite side. Numbers on the curves are values of Dt/l^2 .	58
4.3 Approach to steady-state flow through an infinite plate of thickness L.	59
4.4 Pressure measurement at PLGS during August 2006.	61

FIGURE	PAGE
4.5 The HEP pressure change during the fuelling on August 17 th .	62
4.6 The plot of HEP pressure, boiler load and operating temperature vs. time from Coleson Cove.	64
4.7 The plot of HEP pressure, pH of the solution, boiler blowdown and operating temperature vs. time from Coleson Cove.	64
4.8 The HEP pressure accumulation (Pa/day) vs. the boiler load (MW).	65
4.9 The HEP pressure accumulation (Pa/day) vs. pH of the solution.	66
4.10 The chambers and the diaphragm inside the pressure transducer.	68
4.11 The possibility of hydrogen diffusion through the diaphragm when changing the area of the diaphragm and the highest pressure inside the HEP.	70
4.12 The possibility of hydrogen diffusion through the diaphragm when changing the diaphragm thickness and the total volume of the HEP.	71
4.13 The prediction of hydrogen pressure in the HEP on the pressure accumulation using PLGS parameters (cartesian coordinates).	72
4.14 The prediction of hydrogen pressure in the HEP on the pressure accumulation using Loop 1 parameters (cylindrical coordinate).	72
4.15 The prediction of curving behaviour of the pressure rise using PLGS.	73
4.16 The prediction of curving behaviour of the pressure rise (Loop 1).	73
4.17 The plot of the HEP pressure from PLGS (McKeen <i>et al.</i> , 2007).	74
4.18 Non-linearity of hydrogen pressure from PLGS.	74
4.19 Non-linearity of hydrogen pressure from Loop 1.	75
4.20 The plot of HEP pressure from the experiment on Loop 1 during Oct., 9 th and Oct., 15 th 2007.	76
4.21 The plot of the HEP pressure and hydrogen flux vs. time from Loop 1.	77
4.22 The plot of the rate of pressure rise and the solution temperature vs. time from Loop 1.	77

FIGURE		PAGE
4.23	The plot of HEP pressure from the experiment on Loop 1 during Oct., 9th and Oct., 15th 2007.	78
4.24	The curving of the hydrogen pressure rise from Loop 1.	80
4.25	The effect of solution temperature on the HEP performance.	81
4.26	The HEP pressure rise during addition of dissolved oxygen into the solution at 80 °C.	82
B.1	The hydrogen diffusivity of the carbon steel pipe at PLGS calculated by using the Time-Lag method.	97
F.1	Carbon steel tube used in the hydrogen permeation experiment.	103

ABBREVIATIONS

AECL	Atomic Energy of Canada Limited
ASME	American Standard of Material Engineering
BCC	Body-Centered Cubic
CANDU	Canada Deuterium Uranium
CC	Coleson Cove Generating Station
CNER	Centre for Nuclear Energy Research
COG	CANDU [®] Owners Group Inc.
FAC	Flow-Accelerated (Assisted) Corrosion
FCC	Fac-Centered Cubic
FOLTM	Feeder On-Line Thickness Monitor
HE	Hydrogen Embrittlement
HEP	Hydrogen Effusion Probe
HIC	Hydrogen-Induced Cracking
HMT	Hydrogen Microprint Technique
NTP	Normal Temperature and Pressure
PLGS	Point Lepreau Generating Station
SEM	Scanning Electron Microscope
STP	Standard Temperature and Pressure

LIST OF SYMBOLS

ϕ	Permeability
ϕ_0	Maximum permeability
Δ	Delta operator or difference operator
∇	Del operator or vector differential operator
ρ_{Fe}	Density of iron
ν_i	Stoichiometric coefficient
α	Thermal expansion coefficient
Π	Total pressure of the system
a	Conversion of days to year
A	Diffusion area
c	Concentration of the diffusing substance
C	Corrosion rate
C_0	Concentration in the membrane
C_1	Concentration on the membrane surface at $x=0$
C_2	Concentration on the membrane surface at $x=l$
C_{gas}	Concentration of gas in the solvent
C_p	Constant-pressure specific heat capacity on a mass basis
D	Diffusion coefficient or Diffusivity
D_0	Maximum diffusion coefficient (at infinite temperature)
E_a	Activation energy
E_ϕ	Activation energy of permeability
E_D	Activation energy of diffusivity
E_S	Activation energy of solubility
ΔG^0	Standard Gibb free energy
ΔG^f	Standard Gibb free energy of formation
ΔH^0	Standard heat of reaction
ΔH^f	Standard enthalpy of formation
H_{O_2}	Henry's constant for oxygen in water

J	Diffusion flux or the quantity of substance per area per time
k	Rate constant of chemical reactions
k_0	Pre-exponential factor
K	Equilibrium constant
l	Thickness of substance
L	Length of substance
M_1	Molar mass of the first gas
M_2	Molar mass of the second gas
M_{Fe}	Molar mass of iron
n	Mole
$\frac{\partial n}{\partial t}$	Daily accumulation of hydrogen molecules
p	Partial pressure
P	Pressure
P_∞	Steady-state rates of hydrogen permeation
p_i°	Vapor pressure of the solvent
$\frac{\partial P}{\partial T}$	Rate of pressure increase
pmol	Picomole or one trillionth (10^{-12}) of a mole.
q	Total amount of the gas permeated the membrane
Q	Amount of the gas permeated the membrane per unit area
R	Gas constant
rate1	Rate of effusion of the first gas
rate2	Rate of effusion for the second gas
s	Solubility
S	Solubility constant or concentration per unit of pressure
S_0	Maximum solubility
t	Time
T	Temperature
T_{C1}	Critical temperature of the solvent
T_{eff}	Effective temperature
t_l	Time lag

T_R	Reduced temperature
V	Volume of an HEP
x	Coordinate chosen perpendicular to the reference surface
x_{O_2}	Mole fraction of oxygen in oxygen-saturated water
y_{O_2}	Mole fraction of oxygen in gas phase